Analysis of the effect of a rectangular cavity resonator on acoustic wave transmission in a waveguide

R. Porter*, D.V. Evans

School of Mathematics, University Walk, University of Bristol, BS8 1TW, UK.

Abstract

The transmission of acoustic waves along a two-dimensional waveguide which is coupled through an opening in its wall to a rectangular cavity resonator is considered. The resonator acts as a classical band-stop filter, significantly reducing acoustic transmission across a range of frequencies. Assuming wave frequencies below the first waveguide cut-off, the solution for the reflected and transmitted wave amplitudes is formulated exactly within the framework of inviscid linear acoustics. The main aim of the paper is to develop an approximation in closed form for reflected and transmitted amplitudes when the gap in the thin wall separating the waveguide and the cavity resonator is assumed to be small. This approximation is shown to accurately capture the effect of all cavities resonances, not just the fundamental Helmholtz resonance. It is envisaged this formula (and more generally the mathematical approach adopted) could be used in the development of acoustic metamaterial devices containing resonator arrays.

Keywords: Cavity resonator, acoustic waveguide, integral equations, small-gap approximation

1. Introduction

The Helmholtz resonator is a well-known acoustical device in which a volume of air inside a rigid vessel is made to resonate by exciting acoustic oscillations at its mouth. The original formula for the fundamental resonant frequency ω_h due to Helmholtz was later generalised by Rayleigh [1] and can

*Corresponding author

Email addresses: richard.porter@bris.ac.uk (R. Porter), d.v.evans@bris.ac.uk (D.V. Evans)

be expressed as

$$\omega_h \approx c_s \sqrt{\frac{S}{VL'}} \tag{1.1}$$

where c_s is the wave speed in the acoustic medium, S is the area of the mouth which is assumed to be attached to the resonator body of volume V through a neck of length L. Here $L' = L + l$ is an effective neck length which takes account of added inertia effects and is dependent on the geometry of the neck (often determined semi-empirically and proportional to $S^{1/2}$). The formula above (also see Kinsler *et al.* [2, §10.8] or Chanaud [3]) is approximate, based on the long-wavelength assumption: $\lambda \gg (L', S^{1/2}, V^{1/3})$. It assumes the mass of air in the neck acts mechanically as an incompressible piston connecting the oscillatory pressure at the mouth to the compressible volume of trapped air in the vessel, which in turn acts as a spring.

When a Helmholtz resonator is connected to the wall of a pipe along which acoustic waves are propagating the combined effect can be to drastically alter the acoustic output from total to zero acoustic transmission. This effect is well known and has been exploited, for example, by the automotive industry in engine exhaust systems to suppress noise or improve engine performance. For example, Kinsler *et al.* [2, §10.11] and Chen *et al.* [4] derive the following formula for the coefficient of transmitted power, $|T|^2$, for a wave of frequency ω propagating along a pipe of cross sectional area $A \ll \lambda$ attached to a Helmholtz resonator:

$$|T|^2 \approx \frac{1}{1 + \left(\dfrac{c_s/2A}{\omega L'/S - c_s^2/\omega V} \right)^2}. \tag{1.2}$$

(This formula is also derived on a long wavelength assumption, ignoring the diffractive effect of the relatively small mouth of the resonator.) It shows that there is a significant reduction in acoustic transmission over a broad range of frequencies around $\omega = \omega_h$ where $|T| = 0$. On account of the analogy with mechanical systems used to develop (1.2), there also exists an analogy with electronic circuitry where the effect of Helmholtz resonators can be reproduced with inductors and capacitors to form a band-stop filter (e.g. Montgomery *et al.* [5]).

Helmholtz resonators are used in many applications beyond those already mentioned above, for example in quantum, microwave and optical waveguides (e.g. Shao *et al.* [6], Xu *et al.* [7] and Scharstein [8]). In the theory of water waves, flat-bottomed harbours with small entrances form Helmholtz resonators. This gives rise to the so-called "harbour paradox"

– see Mei [9] who considered a rectangular harbour connected to a semi-infinite ocean through a small gap in a thin wall – in which the smaller the entrance to the harbour the stronger the resonant effect within it.

More recently, Helmholtz resonators have been used extensively in the development of so-called metamaterials and metasurfaces. Thus arrays of sub-wavelength cavities can produce surprising effects upon the macroscopic wave field that are not manifested in naturally-occuring materials. For examples, see Richoux and Pagneaux [10], Fang *et al.* [11], Wang *et al.* [12], Seo *et al.* [13] and Faure *et al.* [14].

The formulae produced in (1.1) and (1.2) above are approximate and are presumably sufficiently accurate for many applications. However, as highlighted by Chanaud [3], they are only appropriate under a long-wavelength assumption and neglect the effects of higher resonant frequencies. The work in this paper – set in the context of two-dimensional acoustics – is aimed at producing an accurate prediction of the transmitted acoustic wave energy in closed form based upon the solutions of the exact equations of linearised acoustics and without making a long-wavelength assumption from the outset. The need to such resolve higher resonant frequencies and accurately encode their effects in scattering coefficients has recently been highlighted in an sound absorption applications of Romero-García *et al.* [15] and Jiménez *et al.* [16].

In the particular problem considered here an incident acoustic wave propagates along a uniform waveguide and interacts with a rectangular cavity through an opening in the waveguide wall. The wall between the waveguide and the cavity is assumed thin so there is no length L assigned to the neck of the resonator. In Section 2 the solution to the problem posed is formulated in terms of integral equations. Solutions are expressed in terms of a series of prescribed functions as a practical means of determining numerical solutions to the integral equations. This forms the basis of the approximate solution for a small gap which is described in Section 3 and relies on some complicated technical details contained in Appendices A and B. The approach here has some similarities with recent work of the authors (see Evans & Porter [17]) in a related problem involving approximating the effect of small gaps on waves. It also shares similarities with the approach taken by Scharstein [8]) in a related problem in which the cavity is excited by plane waves from a semi-infinite domain. An alternative approach here could have been to use the method of matched asymptotic expansions as in Mei [9] by connecting solutions to an inner problem in the vicinity of the gap to an outer solution in which the gap acts as a point source. The outcome of the two approaches have much in common although our central positioning of the gap within

the cavity introduces difficulties avoided by Mei [9] who considered only off-centre gaps. Recent unpublished work (Prof. David Abrahams, personal communication) has followed this approach.

By using our new approximation for small gaps in the long wavelength limit we shall also be able to derive an explicit expression for L' (or l) in (1.1) for the geometry under consideration. The result is not a simple linear scaling with gap size as is commonly assumed. In addition to making the connection with the Helmholtz resonance, Section 4 describes the effect that higher-order cavity resonances have on $|T|$. In Section 5 we present numerical results which test the new approximation against computations based on the exact formulation. Finally in Section 6 we summarise the paper and suggest how this work could be used elsewhere.

2. Exact treatment of the problem

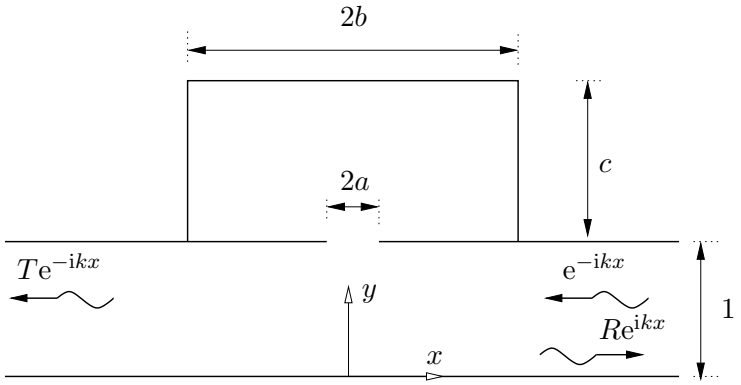

Figure 1: Sketch of channel and connection to cavity via a gap in the channel wall. Waves come from $+\infty$.

2.1. Formulation

An infinitely-long waveguide has parallel acoustically-hard walls along $y = 0$ and $y = 1$ for $-\infty < x < \infty$. A small gap in the wall $y = 1$ extends from $x = -a$ to $x = a$ and connects the waveguide symmetrically to a rectangular basin or cavity of width $2b$ and height c (see Figure 1). All lengths are considered dimensionless, having being scaled by the channel width. The acoustic pressure is written $\Re\{\phi(x, y)e^{-i\omega t}\}$ having angular frequency ω and $\phi(x, y)$ satisfies the wave equation

$$(\nabla^2 + k^2)\phi = 0 \tag{2.1}$$

where $k = \omega/c$, c being the wave speed, and we assume $k < \pi$ throughout so that the frequency is below the first waveguide cut-off. That is, only one propagating wave mode is allowed in the channel.

On all of the acoustically-hard walls, the derivative of ϕ normal to the walls must vanish.

An incident wave of unit amplitude is assumed to have propagated from $x = +\infty$. Thus the far field form of ϕ can be written

$$\phi(x,y) \approx \begin{cases} \mathrm{e}^{-\mathrm{i}kx} + R\mathrm{e}^{\mathrm{i}kx}, & x \to \infty, \\ T\mathrm{e}^{-\mathrm{i}kx}, & x \to -\infty \end{cases} \tag{2.2}$$

where R and T represent the complex reflection and transmission coefficients satisfying the energy relation $|R|^2 + |T|^2 = 1$ as no dissipation is included in the problem.

On account of the symmetry about $x = 0$ in the geometry, we are able to write

$$\phi = \tfrac{1}{2}(\phi^s + \phi^a) \tag{2.3}$$

where $\phi^s(x,y) = \phi^s(-x,y)$ and $\phi^a(x,y) = -\phi^a(-x,y)$. The functions $\phi^{s,a}$ now only need to be found in $x > 0$ when supplemented with the boundary conditions

$$\phi^s_x(0,y) = \phi^a(0,y) = 0. \tag{2.4}$$

If we assume

$$\phi^{s,a}(x,y) \approx \mathrm{e}^{-\mathrm{i}kx} + R^{s,a}\mathrm{e}^{\mathrm{i}kx} \tag{2.5}$$

as $x \to \infty$ it must follow that $|R^{s,a}| = 1$ and that

$$R = \tfrac{1}{2}(R^s + R^a), \qquad T = \tfrac{1}{2}(R^s - R^a). \tag{2.6}$$

2.2. Solution of the symmetric problem

We consider the solution for the function $\phi^s(x,y)$ first. Within the waveguide $0 < y < 1$ we define the Fourier cosine transform

$$\Phi^s(\alpha,y) = \int_0^\infty (\phi^s(x,y) - 2\cos kx)\cos\alpha x \,\mathrm{d}x \tag{2.7}$$

(the function $\phi^s(x,y) - 2\cos kx$ is even and is outgoing as $x \to \infty$). If $u^s(x) \equiv \phi^s_y(x,1)$ over the gap $0 < x < a$ and we define

$$U^s(\alpha) = \int_0^a u^s(\xi)\cos\alpha\xi \,\mathrm{d}\xi \tag{2.8}$$

then the solution in terms of transform variables is easily found to be

$$\Phi^s(\alpha, y) = \frac{U^s(\alpha)\cosh\gamma y}{\gamma\sinh\gamma} \tag{2.9}$$

where $\gamma = \sqrt{\alpha^2 - k^2} \equiv -\mathrm{i}\sqrt{k^2 - \alpha^2}$.

Inverting the transform gives

$$\phi^s(x, y) = 2\cos kx + \frac{2}{\pi}\int_0^\infty \frac{\cosh\gamma y\cos\alpha x}{\gamma\sinh\gamma}\int_0^a u^s(\xi)\cos\alpha\xi\,\mathrm{d}\xi\,\mathrm{d}\alpha \tag{2.10}$$

and the contour of integration is defined to pass under the pole $\alpha = k$ on the real axis. Writing

$$\cos\alpha x\cos\alpha\xi = \tfrac{1}{4}(\mathrm{e}^{\mathrm{i}\alpha(x+\xi)} + \mathrm{e}^{-\mathrm{i}\alpha(x+\xi)} + \mathrm{e}^{\mathrm{i}\alpha(x-\xi)} + \mathrm{e}^{-\mathrm{i}\alpha(x-\xi)}) \tag{2.11}$$

and letting $x \to \infty$ we find, by deforming contours into the upper and lower half-planes where appropriate and collecting residues for those contours deformed upwards, that

$$\phi^s(x, y) \approx 2\cos kx + \frac{\mathrm{i}}{k}\mathrm{e}^{\mathrm{i}kx}\int_0^a u^s(\xi)\cos k\xi\,\mathrm{d}\xi \tag{2.12}$$

and comparing with (2.5), we have

$$R^s = 1 + \frac{\mathrm{i}}{k}\int_0^a u^s(\xi)\cos k\xi\,\mathrm{d}\xi. \tag{2.13}$$

We can return to (2.10) and re-write it as a real principal-value integral plus the contribution from a small semi-circular contour deformed around the pole which is related to (2.13) so that we eventually obtain

$$\phi^s(x, y) = (1 + R^s)\cos kx + \frac{2}{\pi}\int_0^\infty \frac{\cosh\gamma y\cos\alpha x}{\gamma\sinh\gamma}\int_0^a u^s(\xi)\cos\alpha\xi\,\mathrm{d}\xi\,\mathrm{d}\alpha. \tag{2.14}$$

Next we turn our attention to the cavity and express a general solution in terms of a separable series as

$$\phi^s(x, y) = -\sum_{n=0}^{\infty} b_n^s \frac{\cosh\gamma_n^s(1 + c - y)}{\gamma_n^s\sinh\gamma_n^s c}\cos\alpha_n^s x$$

for $0 < x < b$, $1 < y < 1 + c$ where $\alpha_n^s = n\pi/b$ and $\gamma_n^s = \sqrt{{\alpha_n^s}^2 - k^2} = -\mathrm{i}\sqrt{k^2 - {\alpha_n^s}^2}$. Then

$$\phi_y^s(x, 1) = \sum_{n=0}^{\infty} b_n^s\cos\alpha_n^s x = \begin{cases} 0, & a < x < b, \\ u^s(x), & 0 < x < a \end{cases}$$

and so

$$b_n^s = \frac{\epsilon_n}{b}\int_0^a u^s(\xi)\cos\alpha_n^s\xi\,\mathrm{d}\xi$$

where $\epsilon_0 = 1$, $\epsilon_n = 2$ for $n \geq 1$. Thus

$$\phi^s(x,y) = -\sum_{n=0}^{\infty}\frac{\epsilon_n\cosh\gamma_n^s(1+c-y)}{\gamma_n^s b\sinh\gamma_n^s c}\cos\alpha_n^s x\int_0^a u^s(\xi)\cos\alpha_n^s\xi\,\mathrm{d}\xi. \quad (2.15)$$

The final part of the solution is to match $\phi^s(x,y)$ along the opening between the waveguide and the cavity, $y = 1$ for $0 < x < a$ from above and below. This results in the integral equation

$$\int_0^a u^s(\xi)L^s(x,\xi)\,\mathrm{d}\xi = -(1+R^s)\cos kx, \qquad 0 < x < a$$

where we have defined the real-valued kernel

$$\begin{aligned} L^s(x,\xi) &= \frac{2}{\pi}\int_0^{\infty}\frac{\coth\gamma}{\gamma}\cos(\alpha x)\cos(\alpha\xi)\,\mathrm{d}\alpha \\ &\quad + \sum_{n=0}^{\infty}\frac{\epsilon_n\coth\gamma_n^s c}{\gamma_n^s b}\cos(\alpha_n^s x)\cos(\alpha_n^s\xi). \end{aligned} \quad (2.16)$$

Now we write $u^s(x) = -(1+R^s)v^s(x)$ so that

$$\int_0^a v^s(\xi)L^s(x,\xi)\,\mathrm{d}\xi = \cos kx, \qquad 0 < x < a \quad (2.17)$$

and $v^s(x)$ is therefore real. Returning to (2.13) with the rescaling of u^s we find

$$R^s - 1 = -\frac{\mathrm{i}}{k}(R^s+1)C^s, \qquad \text{where} \qquad C^s = \int_0^a v^s(x)\cos kx\,\mathrm{d}x \quad (2.18)$$

is real so that

$$R^s = \frac{(1-\mathrm{i}C^s/k)}{(1+\mathrm{i}C^s/k)} \quad (2.19)$$

and $|R^s| = 1$ as required.

2.3. Numerical solution for the symmetric problem

The numerical approximation of R^s in (2.19) is achieved by first substituting the series solution

$$v^s(x) \approx \tilde{v}^s(x) = \sum_{p=0}^{P} a_p^s v_{2p}(x/a), \qquad v_{2p}(s) = \frac{2(-1)^p T_{2p}(s)}{\pi\sqrt{1-s^2}} \quad (2.20)$$

into the integral equation (2.17), then multiplying through by $v_{2q}(x/a)$, $q = 0, 1, \ldots, P$ and integrating over $0 < x < a$, a process characteristic of the Galerkin method. Here T_n are Chebychev polynomials. The inverse square-root incorporated into the functions $v_{2p}(s)$ ensure the behaviour of the field variable local to the end of the barrier is satisfied automatically. The result is the system of equations

$$\sum_{p=0}^{P} a_p^s L_{pq}^s = J_{2q}(ka), \qquad q = 0, 1, \ldots, P \tag{2.21}$$

where

$$L_{pq}^s = \frac{2}{\pi} \int_0^\infty \frac{\coth \gamma}{\gamma} J_{2p}(\alpha a) J_{2q}(\alpha a)\, \mathrm{d}\alpha + \sum_{n=0}^{\infty} \frac{\epsilon_n \coth \gamma_n^s c}{\gamma_n^s b} J_{2p}(\alpha_n^s a) J_{2q}(\alpha_n^s a) \tag{2.22}$$

which has used the identity (Gradshteyn and Ryzhik [18, §7.355(1)])

$$J_{2p}(l) = \int_0^1 v_{2p}(\xi) \cos(l\xi)\, \mathrm{d}\xi \tag{2.23}$$

and J_n is a Bessel function. Finally, using (2.20) in (2.18) gives

$$C^s \approx \sum_{p=0}^{P} a_p^s J_{2p}(ka). \tag{2.24}$$

2.4. Solution of the antisymmetric problem

Next we briefly consider the antisymmetric problem. For $0 < y < 1$ we define

$$\Phi^a(\alpha, y) = \int_0^\infty (\phi^a(x, y) + 2\mathrm{i} \sin kx) \sin \alpha x\, \mathrm{d}\alpha$$

since $\phi^a(x, y) + 2\mathrm{i} \sin kx$ is outgoing at infinity and find

$$\Phi^a(\alpha, y) = \frac{U^a(\alpha) \cosh \gamma y}{\gamma \sinh \gamma}$$

as before where

$$U^a(\alpha) = \int_0^a u^a(x) \sin \alpha x\, \mathrm{d}x$$

in terms of $u^a(x) \equiv \phi_y^a(x, 1)$ across $0 < x < a$. Following the methods outlined in the symmetric case leads to the representation

$$\phi^a(x, y) = -\mathrm{i}(1 - R^a) \sin kx + \frac{2}{\pi} \int_0^\infty \frac{\cosh \gamma y \sin \alpha x}{\gamma \sinh \gamma} \int_0^a u^a(\xi) \sin \alpha \xi\, \mathrm{d}\xi\, \mathrm{d}\alpha. \tag{2.25}$$

Also in a similar manner to before, the solution in the cavity is found to be

$$\phi^a(x,y) = -2\sum_{n=0}^{\infty} \frac{\cosh\gamma_n^a(1+c-y)}{\gamma_n^a b\sinh\gamma_n^a c}\sin\alpha_n^a x\int_0^a u^a(\xi)\sin\alpha_n^a\xi\,\mathrm{d}\xi \qquad (2.26)$$

where $\alpha_n^a = (n+\frac{1}{2})\pi/b$ and $\gamma_n^a = \sqrt{\alpha_n^{a\,2}-k^2} = -\mathrm{i}\sqrt{k^2-\alpha_n^{a\,2}}$.

Matching potentials (2.25), (2.26) across the gap $y=1$ leads to

$$\int_0^a u^a(\xi)L^a(x,\xi)\,\mathrm{d}\xi = \mathrm{i}(1-R^a)\sin kx, \qquad 0<x<a$$

where

$$\begin{aligned} L^a(x,\xi) &= \frac{2}{\pi}\int_0^\infty \frac{\coth\gamma d}{\gamma}\sin(\alpha x)\sin(\alpha\xi)\,\mathrm{d}\alpha \\ &\quad +2\sum_{n=0}^{\infty}\frac{\coth\gamma_n^a c}{\gamma_n^a b}\sin(\alpha_n^a x)\sin(\alpha_n^a\xi). \end{aligned} \qquad (2.27)$$

We write $u^a(x) = \mathrm{i}(1-R^a)v^a(x)$ so that (2.27) becomes

$$\int_0^a v^a(\xi)L^a(x,\xi)\,\mathrm{d}\xi = \sin kx, \qquad 0<x<a \qquad (2.28)$$

and consequently $v^a(x)$ is real. We also find

$$R^a+1 = \frac{\mathrm{i}}{k}(1-R^a)C^a, \qquad C^a = \int_0^1 v^a(x)\sin kx\,\mathrm{d}x \qquad (2.29)$$

so that

$$R^a = -\frac{(1-\mathrm{i}C^a/k)}{(1+\mathrm{i}C^a/k)} \qquad (2.30)$$

and so $|R^a|=1$ as required.

The numerical approximation to R^a is achieved by substituting the series solution

$$v^a(x) \approx \tilde{v}^a(x) = \sum_{p=0}^{P} a_p^a v_{2p+1}(x/a), \qquad v_{2p+1}(s) = \frac{2(-1)^p T_{2p+1}(s)}{\pi\sqrt{1-s^2}} \qquad (2.31)$$

into the integral equation (2.28), then multiplying through by $v_{2q+1}(x/a)$, $q=0,1,\ldots,P$ and integrating over $0<x<a$ to give

$$\sum_{p=0}^{P} a_p^a L_{pq}^a = J_{2q+1}(ka), \qquad q=0,1,\ldots,P \qquad (2.32)$$

where

$$L^a_{pq} = \frac{2}{\pi}\int_0^\infty \frac{\coth\gamma}{\gamma} J_{2p+1}(\alpha a)J_{2q+1}(\alpha a)\,\mathrm{d}\alpha + 2\sum_{n=0}^{\infty} \frac{\coth\gamma^a_n c}{\gamma^a_n b} J_{2p+1}(\alpha^a_n a)J_{2q+1}(\alpha^a_n a) \tag{2.33}$$

which uses the identity (Gradshteyn and Ryzhik [18, §7.355(2)])

$$J_{2p+1}(l) = \int_0^1 v_{2p+1}(\xi)\sin(l\xi)\,\mathrm{d}\xi \tag{2.34}$$

whilst (2.31) in (2.29) gives

$$C^a \approx \sum_{p=0}^{P} a^a_p J_{2p+1}(ka). \tag{2.35}$$

2.5. Accelerating convergence of the integrals

For numerical purposes, it helps to accelerate the convergence of the integrals in the definitions (2.22), (2.33) used in the algebraic systems of equations. For p, q not both equal to zero, we may write

$$\frac{2}{\pi}\int_0^\infty \left(\frac{\coth\gamma}{\gamma} - \frac{1}{\alpha}\right) J_p(\alpha a)J_q(\alpha a)\,\mathrm{d}\alpha + \frac{1}{\pi}\frac{\delta_{pq}}{p} \tag{2.36}$$

whilst for $p = q = 0$ we can write

$$\frac{2}{\pi}\int_0^\infty \left(\frac{\coth\gamma}{\gamma} - \frac{\alpha}{\alpha^2 + l^2}\right) J_0^2(\alpha a)\,\mathrm{d}\alpha + \frac{2}{\pi} I_0(la)K_0(la) \tag{2.37}$$

(for any l); see Gradshteyn and Ryzhik [18, §6.538(2), §6.541(1)]).

In each case the rate of decay of the integrand with α is increased from $O(\alpha^{-2})$ to $O(\alpha^{-3})$. These formulae may be used in the first kind system of equations (2.21) and (2.32) to convert them into 2nd kind equations. The process of removing the leading order term to accelerate the convergence of the integral resulting in the transformation from first kind to second kind is indicative of removing the dominant logarithmic behaviour which reside in the kernels L^s and L^a.

3. A small-gap approximation

The remainder of the paper focusses on developing an approximation to the solution based on the assumption $a \ll 1$. The purpose is two-fold: (i) to provide simplified explicit expressions which accurately capture the behaviour of the reflection coefficient; and (ii) to help explain the qualitative features of the results.

As $a \to 0$ the solution is increasingly dominated by the first term in the series used in the Galerkin approximation and we truncate at $P = 0$ as a leading-order approximation to the solution when $a \ll 1$. It follows that

$$C^s \approx J_0^2(ka)/L_{00}^s \approx 1/L_{00}^s \tag{3.1}$$

using $J_0(ka) \approx 1 + O(a^2)$ for $a \ll 1$ where

$$L_{00}^s = \frac{2}{\pi} \int_0^\infty \frac{\coth \gamma}{\gamma} J_0^2(\alpha a)\, \mathrm{d}\alpha - \frac{\cot kc}{kb} + 2 \sum_{n=1}^{\infty} \frac{\coth \gamma_n^s c}{\gamma_n^s b} J_0^2(\alpha_n^s a). \tag{3.2}$$

Similarly, using a $P = 0$ truncation to approximate the small-gap solution to the antisymmetric problem we have

$$C^a \approx J_1^2(ka)/L_{00}^a \approx \tfrac{1}{4} k^2 a^2 / L_{00}^a \tag{3.3}$$

where

$$L_{00}^a = \frac{2}{\pi} \int_0^\infty \frac{\coth \gamma}{\gamma} J_1^2(\alpha a)\, d\alpha + 2 \sum_{n=0}^{\infty} \frac{\coth \gamma_n^a c}{\gamma_n^a b} J_1^2(\alpha_n^a a). \tag{3.4}$$

It is tempting to set $C^a \approx 0$ (and hence $R^a \approx -1$) to be consistent with the neglect of $O(a^2)$ terms in the symmetric problem. However, C^a can be significant if L_{00}^a is at least as small as $O(a^2)$, a situation which cannot be disregarded as we shall see.

To be consistent with approximating the numerators of (3.1) and (3.3) under the assumption $a \ll 1$, we also consider the $a \ll 1$ approximation to L_{00}^s and L_{00}^a. Thus, using the relation (2.23) we have

$$L_{00}^s = \frac{4}{\pi^2} \int_0^1 \frac{\mathrm{d}s}{\sqrt{1-s^2}} \int_0^1 \frac{\mathrm{d}t}{\sqrt{1-t^2}} L^s(as, at). \tag{3.5}$$

The approximation to $L^s(as, at)$ for $a \ll 1$ is derived in Appendix A and results in

$$L^s(as, at) \approx -\frac{2}{\pi} \ln |s^2 - t^2| + A^s \tag{3.6}$$

up to terms of $O(a^2)$ where A^s is given in (A.10). Substituting (3.6) into (3.5) and using $n = 0$ in the following general result involving Chebychev polynomials

$$\int_{-1}^{1} \frac{T_n(t) \ln|s-t|}{\sqrt{1-t^2}}\,\mathrm{d}t = \begin{cases} -\pi \ln(2), & n = 0 \\ -\pi T_n(s)/n, & n \geq 1 \end{cases} \tag{3.7}$$

(Gradshteyn and Ryzhik [18, §4.292(1), §7.344(1)]) to perform the integration required, results in

$$L^s_{00} \approx \frac{4}{\pi} \ln(2) + A^s. \tag{3.8}$$

Thus, according to (3.1) we have

$$C^s \approx \frac{1}{A^s + (4/\pi)\ln(2)} \equiv \frac{1}{Q^s} \tag{3.9}$$

such that

$$Q^s = -\frac{2}{\pi} \ln\left(\frac{\pi^2 a^2}{4b}\right) - \frac{\cot kc}{kb} + 2\sum_{n=1}^{\infty} \left(\frac{\coth \gamma_n^s c}{\gamma_n^s b} + \frac{1}{k_n} - \frac{2}{n\pi}\right). \tag{3.10}$$

Turning to the antisymmetric problem, in a similar manner we can use (2.34) to express (3.4) as

$$L^a_{00} = \frac{4}{\pi^2} \int_0^1 \frac{s\,\mathrm{d}s}{\sqrt{1-s^2}} \int_0^1 \frac{t\,\mathrm{d}t}{\sqrt{1-t^2}} L^a(as, at). \tag{3.11}$$

In Appendix B it is shown that

$$L^a(as, at) \approx -\frac{2}{\pi} \ln\left(\frac{|s-t|}{|s+t|}\right) + a^2 G(s,t) \tag{3.12}$$

for $a \ll 1$ where G is defined by (B.12). Subsituting (3.12) into (3.11) with (B.12) and, noting the definitions of the first few Chebychev polynomials $T_0(x) = 1$, $T_1(x) = x$, $T_2(x) = 2x^2 - 1$ and $T_3(x) = 4x^3 - 3x$, we have

$$\begin{aligned} L^a_{00} \approx \frac{4}{\pi^2} \int_0^1 \frac{s}{\sqrt{1-s^2}} \Bigg[& -\frac{2}{\pi} \int_{-1}^{1} \frac{T_1(t) \ln|s-t|}{\sqrt{1-t^2}}\,\mathrm{d}t + sA^a a^2 \frac{\pi}{4} \\ & + \frac{k^2 a^2}{2\pi} s^2 \int_{-1}^{1} \frac{T_1(t) \ln|s-t|}{\sqrt{1-t^2}}\,\mathrm{d}t + \frac{k^2 a^2}{2\pi} \int_{-1}^{1} \frac{(\frac{1}{4}T_3(t) + \frac{3}{4}T_1(t)) \ln|s-t|}{\sqrt{1-t^2}}\,\mathrm{d}t \\ & - \frac{k^2 a^2}{\pi} s \int_{-1}^{1} \frac{(\frac{1}{2}T_2(t) + \frac{1}{2}T_0(t)) \ln|s-t|}{\sqrt{1-t^2}}\,\mathrm{d}t \Bigg] ds \end{aligned}$$

after using the odd and evenness of functions to extend the range of integration to the interval $(-1,1)$.

Using the result (3.7) gives

$$\begin{aligned} L^a_{00} \approx \frac{4}{\pi^2}\int_0^1 \frac{s}{\sqrt{1-s^2}}\Big[2T_1(s)+\tfrac{1}{4}T_1(s)A^a a^2\pi - k^2a^2(\tfrac{1}{8}T_3(s)+\tfrac{3}{8}T_1(s)) \\ -k^2a^2\left(\tfrac{1}{24}T_3(s)+\tfrac{3}{8}T_1(s)\right)\Big) + k^2a^2(\tfrac{1}{2}(2s^3-s)+\tfrac{1}{2}s\ln(2))\Big]\,\mathrm{d}s \\ = \frac{2}{\pi}+\frac{A^a a^2}{4}-\frac{k^2a^2}{2\pi}(1-\ln(2)) \end{aligned}$$

after first converting powers of s into Chebychev polynomials and then using the orthogonality of the Chebychev polynomials. Thus (3.3) gives,

$$C^a \approx \frac{\frac{1}{8}\pi k^2a^2}{1+\frac{1}{8}\pi k^2a^2Q^a} \tag{3.13}$$

where

$$\begin{aligned} Q^a = \frac{A^a}{k^2}-\frac{2}{\pi}(1-\ln(2)) = \frac{1}{\pi}-\frac{1}{\pi}\ln\left(\frac{\pi^2a^2}{16b}\right)+\frac{\pi}{12k^2b^2}+\frac{\pi}{6k^2} \\ +\frac{2}{k^2}\sum_{n=0}^{\infty}\left(\frac{{\alpha^a_n}^2\coth\gamma^a_n c}{\gamma^a_n b}-\frac{\alpha^a_n}{b}-\frac{k^2}{2\alpha^a_n b}\right). \end{aligned} \tag{3.14}$$

4. Analysis of cavity resonances

First we make the connection to the approximate formula presented in (1.2) for the Helmholtz resonance. For the geometry assumed in this problem we have $A=1$, $S=2a$, $V=2bc$ whilst $k=\omega/c_s$ and so (1.2) is re-expressed as

$$|T|^2 \approx \frac{1}{1+\dfrac{1}{k^2(L'/a-1/(k^2bc))^2}} \tag{4.1}$$

where $L'=l$ and l is an "effective neck length" which is undetermined.

Using the small-gap approximation developed in §3 we find that

$$|T|^2 = \frac{1}{1+\dfrac{1}{k^2\left(\dfrac{Q^s+\frac{1}{8}\pi a^2(1+k^2Q^aQ^s)}{1+\frac{1}{8}\pi a^2k^2(Q^a-Q^s)}\right)^2}} \tag{4.2}$$

Comparing (4.1) to (4.2) provides an explicit expression for the effective neck length under the small-gap approximation. However, this expression depends upon frequency and it helps to go further and impose assumptions made in determining both (4.1) and (4.2) that $k \ll 1$ and $a \ll 1$. Then from (3.10),

$$Q^s \approx \frac{2}{\pi} \log\left(\frac{4b}{\pi^2 a^2}\right) - \frac{1}{k^2 bc} \tag{4.3}$$

using $\cot kc \approx 1/kc$ for $kc \ll 1$ and assuming c is large enough that $\coth \pi c \approx 1$ to justifying the neglect of the final summation in (3.10). Comparison of (4.2) with (4.1) now shows that the long wavelength approximation to the effective neck length for an opening of width $2a$ into a cavity of width $2b$ through a thin wall into a waveguide of width 1 is

$$L' = l \approx \frac{2a}{\pi} \log\left(\frac{4b}{\pi^2 a^2}\right). \tag{4.4}$$

It follows from (1.1) that the approximate wavenumber $k_h = \omega_h / c_s$ at which the Helmholtz resonance occurs is

$$k_h \approx \sqrt{\frac{\pi}{2bc \log\left(\frac{4b}{\pi^2 a^2}\right)}}. \tag{4.5}$$

We can also describe the effect of the higher-order resonances on characteristics of acoustic transmission. Thus, we can re-write expressions for Q^s and Q^a using the following result

$$\frac{\coth z}{z} = \sum_{m=0}^{\infty} \frac{\epsilon_m}{m^2\pi^2 + z^2}$$

(e.g. Gradshteyn and Ryzhik [18, §1.421(4)]). Thus (3.10) may be written,

$$Q^s = -\frac{2}{\pi} \ln\left(\frac{\pi^2 a^2}{4b}\right) - \frac{\cot kc}{kb} + 2\sum_{n=1}^{\infty} \left(\frac{1}{k_n} - \frac{2}{n\pi} + \frac{1}{bc} \sum_{m=0}^{\infty} \frac{\epsilon_m}{(k^s_{m,n})^2 - k^2} \right) \tag{4.6}$$

after using the definition of γ^s_n, where

$$k^s_{m,n} = \pi \sqrt{m^2/c^2 + n^2/b^2}, \tag{4.7}$$

(m, n positive integers, not both zero) are the eigenfrequencies corresponding to natural oscillations, symmetric about $x = 0$, of the closed cavity. Likewise

(3.14) may be written

$$Q^a = \frac{1}{\pi} - \frac{1}{\pi}\ln\left(\frac{\pi^2 a^2}{16b}\right) + \frac{\pi}{12k^2b^2} + \frac{\pi}{6k^2} - \frac{2}{k^2}\sum_{n=0}^{\infty}\left(\frac{\alpha_n^a}{b} + \frac{k^2}{2\alpha_n^a b} - \frac{{\alpha_n^a}^2}{bc}\sum_{m=0}^{\infty}\frac{\epsilon_m}{(k_{m,n}^a)^2 - k^2}\right)$$

where

$$k_{m,n}^a = \pi\sqrt{m^2/c^2 + (n+\tfrac{1}{2})^2/b^2}, \qquad m,n \geq 0. \tag{4.8}$$

Thus expressions for Q^s and Q^a regarded as functions of k are singular at $k = k_{m,n}^s$ and $k_{m,n}^a$ respectively. This behaviour is important in analysing the effect of cavity resonances on the reflection and transmission oefficients.

From (4.2) zero transmission under the small-gap approximation requires $Q^s(1 + \frac{1}{8}\pi k^2 a^2 Q^a) = -\frac{1}{8}\pi a^2$. Assuming $a \ll 1$ this will be satisfied if either

$$Q^s \approx -\frac{\pi a^2}{8}, \qquad \text{or} \qquad Q^a \approx -\frac{8}{\pi k^2 a^2} - \frac{1}{k^2 Q^s}.$$

On the other hand total transmission under the small-gap approximation requires, from (4.2) that $Q^a - Q^s = -8/(\pi a^2 k^2)$ and, again assuming $a \ll 1$ we either have

$$Q^s \approx \frac{8}{\pi k^2 a^2} + Q^a. \qquad \text{or} \qquad Q^a \approx -\frac{8}{\pi k^2 a^2} + Q^s$$

In each cases above, conditions are derived from a single condition supposes that only one of $Q^s(k)$ or $Q^a(k)$ varies rapidly as a function of k which we have previously established as behaviour associated with resonances.

Based on the $a \ll 1$ assumption, there is therefore strong evidence that total transmission and reflection will occur at values of k close to resonant frequencies where $Q^s(k)$ and $Q^a(k)$ undergo rapid variations to $\pm\infty$. Moreover those frequencies at which zeros of R and T associated with the antisymmetric resonances occur will be much closer together than those associated with symmetric resonances. These features will be observed in the numerical results presented shortly.

5. Results

We first take a relatively small cavity with the choice $b = \frac{1}{2}$ and $c = 1$, so that the cavity is square with each side the same length as the channel

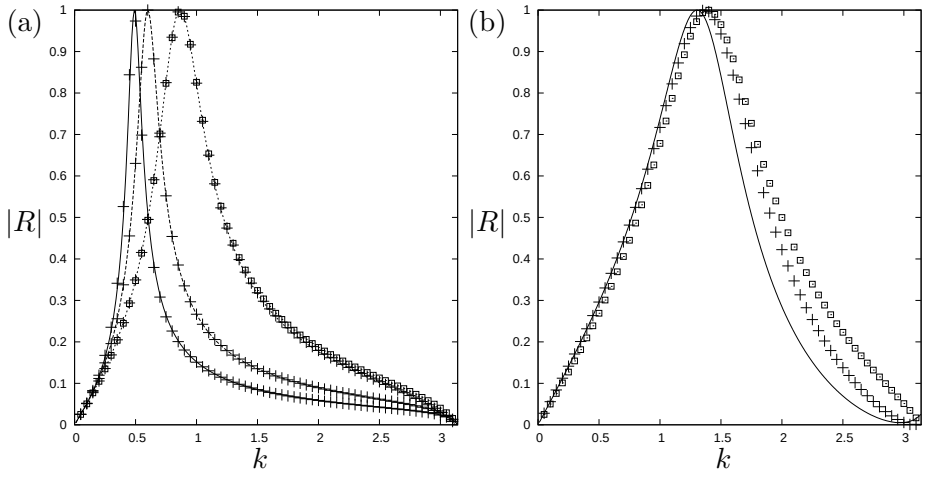

Figure 2: The modulus of the reflection coefficient against k for $b = \frac{1}{2}$, $c = 1$ and (a) $a = 0.001$, 0.01 0.1 (from left to right) and (b) $a = 0.5$. Curves are exact results, + (and □) are full (and symmetric only) asymptotic results for small a.

width. In the numerical scheme, the exact results accurate to at least 5 decimal places are computed using a truncation parameter $P = 3$.

In Figure 2 the four solid curves each represent the exact $|R|$ against k for a different gap ratio a from 0.001 up to 0.5 when the gap in the side wall is the same as the width of the cavity. Alongside each set of curves, the symbols show the results from two versions of small-gap approximation: the crosses showing the full approximation to both C^s and C^a and the boxes when C^a is set to zero (only shown on curves where there is a visible difference). Agreement between the exact results and the small-gap approximation is excellent certainly up to gaps occupying 20% of the width of the cavity. Indeed, they are still impressive for a gap the same width of the cavity, well beyond the range of values where they are expected to work.

As expected, the curves shown in Figure 2 each demonstrate frequencies at which total reflection occurs and correspond to the Helmholtz resonance. We see that total reflection persists when a is reduced to 0.001 and as a is reduced even further it persists with the peak to unity in $|R|$ moving towards $k = 0$ logarithmically slowly. This can be deduced from the formula (4.2) when $Q^s = 0$ and Q^s is given by (4.3) deduced under the long wavelength ($k \ll 1$) assumption.

The values of k at which total reflection occurs in Figure 2 are gven by 0.489, 0.601, 0.866, 1.372 corresponding to the values $a = 0.001$, 0.01, 0.1,

0.5 whilst the values k_h predicted by the formula (4.2) being equivalent to (1.1), are 0.507, 0.642, 1.022 and fails to predict a value for $a = 0.5$. This confirms that (4.2) works in the long wavelength ($k \ll 1$) limit but also highlights that its accuracy and range of applicability is somewhat limited.

In Figure 3 we increase the size of the cavity to $b = 1.2$ and $c = 1.6$ (these values have no particular significance). In the three sub-figures we increase the gap size from $a = 0.01$ in (a) through $a = 0.1$ in (b) to $a = 0.4$ in (c). Again, curves represent the exact numerical computations and the crosses use the approximate formula for a small gap whilst the boxes show the effect of using the approximate formula, but setting $C^a = 0$. As before, the full approximate formula applies well in each case despite the increased complexity of the behaviour of $|R|$. Thus the first broadbanded peak present in Figure 3 is associated with the fundamental Helmholtz mode already discussed. Now there are additional frequencies at which $|R| = 1$ and corresponding frequencies nearby at which $R = 0$ where total transmission occurs. Increasingly evident as a increases is a second set of even more rapid variations in $|R|$ which interlace the first set. As previously discussed in §3.1, these features are manifested by the onset of higher-order resonances in the rectangular cavity. For the example in Figure 3 these occur at $k^a_{1,0} \approx 1.31$, $k^s_{0,1} \approx 1.96$, $k^a_{1,1} \approx 2.36$, $k^s_{2,0} \approx 2.62$. The small-gap approximation illustrated by boxes in Figure 3 in which we set $C^a = 0$ not only fails to capture the antisymmetric resonances but leads to a significant loss in accuracy across a wide range of values of k. Finally in Figure 4 we show the effect of shrinking the cavity by considering a square cavity with $2b = c = 0.5$ down to 0.0625 with a fixed gap size of $a = 0.01$. The sequence of curves illustrate that total reflection due to the Helmholtz mode persists as the size of the cavity tends to zero although it becomes an effect which is squeezed closer to the first channel cut-off frequency $k = \pi$.

6. Conclusions

The principal aim of this paper has been to present a closed form approximation which accurately captures all of the effects that a rectangular cavity resonator connected by a small gap to an acoustic waveguide has on the reflection and transmission coefficients. These coefficients are given by (2.6) with R^s and R^a expressed by (2.19) and (2.30), C^s and C^a being given by (3.9) and (3.13) in terms of Q^s given by (3.10) and Q^a given by (3.14). The results presented here illustrate that the approximation does indeed accurately represent the solution for gap sizes well above 20% of the size of the resonator.

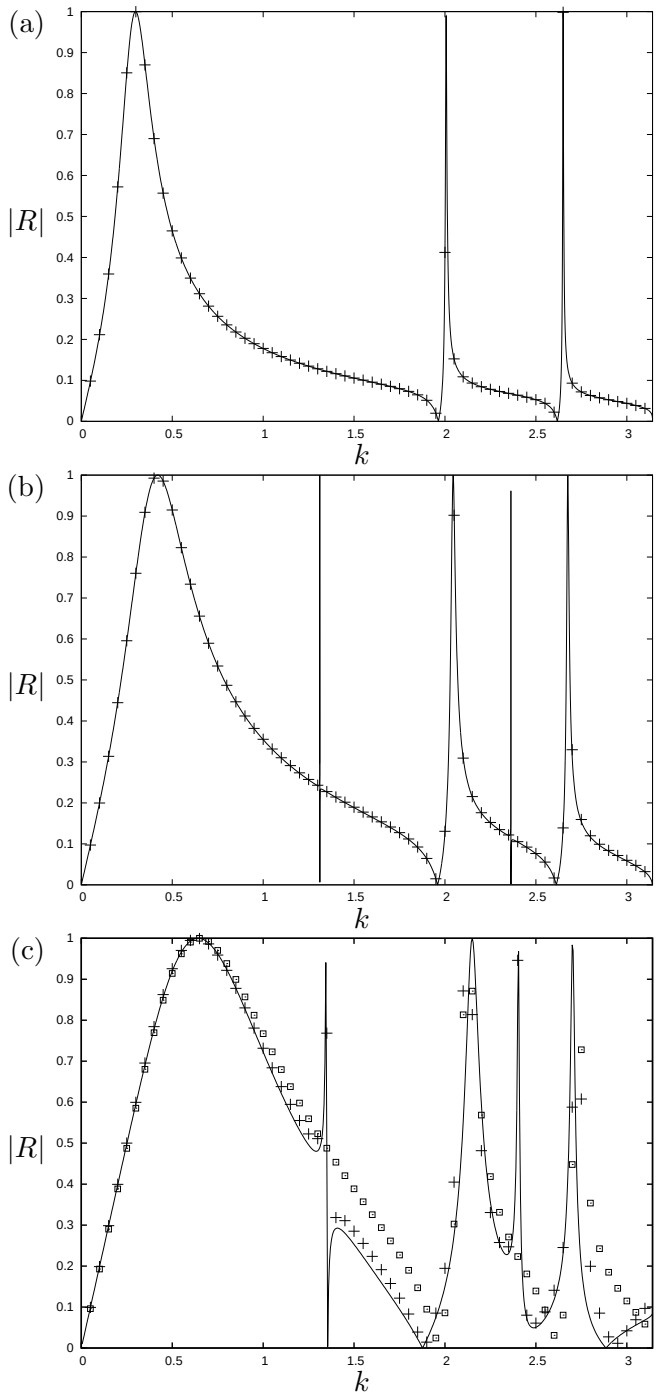

Figure 3: The modulus of the reflection coefficient against k for $b = 1.2$, $c = 1.6$ and: (a) $a = 0.01$; $a = 0.1$; $a = 0.4$. Curves are exact results, $+$ (and $\Box$) are full (and symmetric only) asymptotic results for small a.

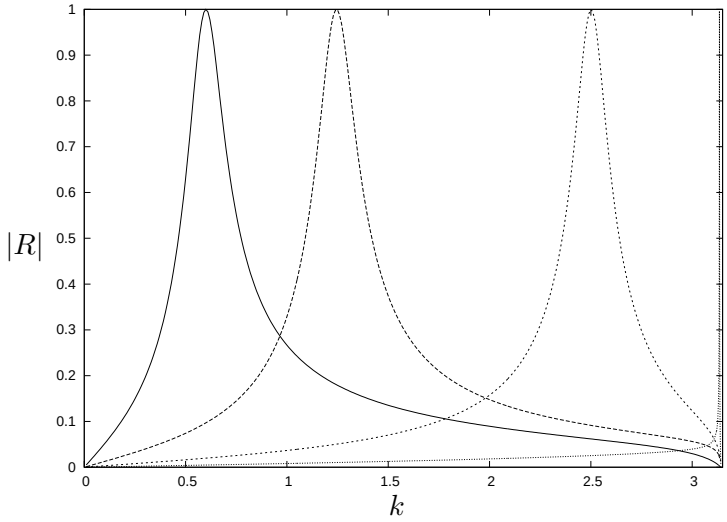

Figure 4: The modulus of the reflection coefficient against k for $a = 0.01$ and a square cavity with dimensions $c = 0.5$, 0.25, 0.125 and 0.0625. (from left to right).

We have also shown how this approximation relates to the long wavelength approximation (1.1) to the Helmholtz resonator and provided an explicit expression (4.4) for the effective neck length. It has also been shown how the effects of higher-order resonances in the cavity are manifested in the behavour of the reflection and transmission coefficients.

The expressions for reflection and transmission coefficients could be used to determine accurate predictions for scattering of acoustic signals by sound absorbing or metamaterial arrays of Helmholtz resonators, as considered in papers cited in the Introduction. The approach taken in the approximation of integral equations for small gaps in cavities could be extended to circular resonators, for example. The inclusion of damping into the dynamics could be also be made. Finally, there is the intriguing possibility that periodic linear arrays of cavity resonators with small gaps embedded in a plane surface bounding a semi-infinite domain could support surface waves.

Appendix A: $a \ll 1$ approximation to the kernel L^s

Starting with the definition (2.16) we write

$$L^s(as, at) = I^s(as, at) + S^s(ax, at) \tag{A.1}$$

where

$$I^s(as,at) = \frac{2}{\pi}\int_0^\infty \frac{\coth\gamma}{\gamma}\cos(\alpha as)\cos(\alpha at)\,\mathrm{d}\alpha = \Re\{I(a(s-t))+I(a(s+t))\} \tag{A.2}$$

with

$$I(X) = \frac{1}{\pi}\int_0^\infty \frac{\coth\gamma}{\gamma}\mathrm{e}^{\mathrm{i}\alpha X}\,d\alpha \tag{A.3}$$

and

$$S^s(as,at) = \sum_{n=0}^{\infty}\frac{\epsilon_n \coth\gamma_n^s c}{\gamma_n^s b}\cos(\alpha_n^s as)\cos(\alpha_n^s at). \tag{A.4}$$

We start by considering the leading order contribution from the integral $I^s(as,at)$ for small a. For $X>0$ we write the integral $I(X)$ as a contour deformed over the pole $\alpha = k$ plus half its residue and then we deform the contour onto the positive imaginary axis where we pick up half residues from the sequence of purely imaginary poles $\alpha = \mathrm{i}k_n$ where $k_n = \sqrt{n^2\pi^2 - k^2}$. For $X<0$ a similar procedure applies by going into the lower half plane. The combined result is

$$I(X) = \frac{\mathrm{i}\mathrm{e}^{\mathrm{i}k|X|}}{2k} + \sum_{n=1}^{\infty}\frac{\mathrm{e}^{-k_n|X|}}{k_n} \tag{A.5}$$

and we can write

$$\begin{aligned}\Re\{I(X)\} \;=\; & -\frac{\sin(k|X|)}{2k} + \sum_{n=1}^{\infty}\left(\frac{\mathrm{e}^{-k_n|X|}}{k_n} - \frac{\mathrm{e}^{-n\pi|X|}}{n\pi}\right)\\ & -\frac{1}{\pi}\ln(2\sinh(\tfrac{1}{2}\pi|X|)) + \tfrac{1}{2}|X|\end{aligned} \tag{A.6}$$

after using the MacLaurin expansion for the logarithm to sum the second infinite series explicitly.

Assuming $a \ll 1$ and retaining terms up to a constant in (A.6), we have from (A.2)

$$I^s(as,at) \approx -\frac{1}{\pi}\ln|s^2-t^2| - \frac{2}{\pi}\ln(\pi a) + 2\sum_{n=1}^{\infty}\left(\frac{1}{k_n} - \frac{1}{n\pi}\right). \tag{A.7}$$

In a similar manner we consider the series $S^s(as,at)$ in (A.4) as $a\to 0$. This is written

$$\begin{aligned}S^s(as,at) \;=\; & -\frac{\cot kc}{kb} + 2\sum_{n=1}^{\infty}\left(\frac{\coth\gamma_n^s c}{\gamma_n^s b} - \frac{1}{n\pi}\right)\cos(\alpha_n^s as)\cos(\alpha_n^s at)\\ & -\frac{1}{\pi}\ln\left(2|\cos(a\pi s/b) - \cos(a\pi t/b)|\right)\end{aligned}$$

using, for example, Jones (1966, p.250) to explicitly sum the second series. So with $a \ll 1$ we have

$$S^s(as,at) \approx -\frac{1}{\pi}\ln|s^2-t^2| - \frac{2}{\pi}\ln\left(\frac{\pi a}{b}\right) - \frac{\cot kc}{kb} + 2\sum_{n=1}^{\infty}\left(\frac{\coth\gamma_n^s c}{\gamma_n^s b} - \frac{1}{n\pi}\right) \tag{A.8}$$

retaining terms up to a constant and neglecting terms $O(a^2)$. Bringing the two results (A.7), (A.8) together,

$$L^s(as,at) \approx -\frac{2}{\pi}\ln|s^2-t^2| + A^s \tag{A.9}$$

for $a \ll 1$ where

$$A^s = -\frac{2}{\pi}\ln\left(\frac{\pi^2 a^2}{b}\right) + 2\sum_{n=1}^{\infty}\left(\frac{1}{k_n} - \frac{1}{n\pi}\right) - \frac{\cot kc}{kb} + 2\sum_{n=1}^{\infty}\left(\frac{\coth\gamma_n^s c}{\gamma_n^s b} - \frac{1}{n\pi}\right). \tag{A.10}$$

Appendix B: $a \ll 1$ approximation to the kernel L^a

We can repeat similar arguments to those used in Appendix A to approximate the $L^a(as,at)$ defined by (2.27) under the assumption $a \ll 1$. Decomposing into integrals and series as in (A.1) with $L^a = I^a + S^a$, we have

$$I^a(as,at) = \Re\{I(a(s-t)) - I(a(s+t))\} \tag{B.1}$$

where I is defined in (A.3) and its real part taken in (A.6). We now retain terms up to $O(a^2)$. Thus, using $\ln(\sinh|x|) \sim \ln|x| + \frac{1}{6}x^2 + O(x^4)$

$$\begin{aligned}\Re\{I(X)\} \;\approx\; & -\frac{1}{\pi}\ln(\pi|X|) - \frac{\pi X^2}{24} \\ & + \sum_{n=1}^{\infty}\left(\frac{\mathrm{e}^{-k_n|X|}}{k_n} - \frac{\mathrm{e}^{-n\pi|X|}}{n\pi} - \frac{k^2}{2(n\pi)^3}\cos(n\pi X)\right) + \frac{k^2}{2\pi^3}V(\pi X)\end{aligned}$$

where we have subtracted and added terms in the series

$$V(\pi X) = \sum_{n=1}^{\infty}\frac{\cos(n\pi X)}{n^3} \approx \zeta(3) - \frac{3}{4}\pi^2X^2 + \frac{1}{2}\pi^2X^2\ln(\pi|X|) + \ldots \tag{B.2}$$

as $X \to 0$ where ζ is the zeta function. This can be deduced from integrating twice the result

$$-\sum_{n=1}^{\infty}\frac{\cos n\pi X}{n} = \frac{1}{2}\ln(2(1-\cos\pi X)) \sim \ln(\pi|X|) + O(X^2)$$

as $X \to 0$ (Gradshteyn and Ryzhik [18, §1.441(2)]). Thus we find

$$\Re\{I(X)\} \approx C_1 - \frac{1}{\pi}\ln(\pi|X|) - \frac{\pi X^2}{24} - \frac{3k^2X^2}{8\pi} + \frac{k^2}{4\pi}X^2\ln(\pi|X|) \qquad \text{(B.3)}$$

where C_1 is a constant which includes both the constant in (B.2) and the series in (B.2) evaluated at $X = 0$.

Using (B.3) in (B.1) finally gives

$$\begin{aligned} I^a(as,at) \approx & -\frac{1}{\pi}\log\left(\frac{|s-t|}{|s+t|}\right) + \frac{\pi a^2 st}{6} + \frac{3k^2a^2st}{2\pi} \\ & + \frac{k^2a^2}{4\pi}\left((s^2+t^2)\log\left(\frac{|s-t|}{|s+t|}\right) - 2st\log\left(\pi^2a^2|s^2-t^2|\right)\right) \end{aligned} \qquad \text{(B.4)}$$

as $a \to 0$. Next we turn to the expression for S^a which we write as

$$S^a(as,at) = S_1^a(as,at) + S_2^a(as,at)$$

where

$$S_1^a(as,at) = 2\sum_{n=0}^{\infty}\left(\frac{\coth\gamma_n^a c}{\gamma_n^a b} - \frac{1}{\alpha_n^a b}\right)\sin(\alpha_n^a as)\sin(\alpha_n^a at)$$

and

$$S_2^a(as,at) = 2\sum_{n=0}^{\infty}\frac{\sin(\alpha_n^a as)\sin(\alpha_n^a at)}{\alpha_n^a b}.$$

Using the definition of α_n^a, this can be arranged as

$$S_2^a(as,at) = \frac{2}{\pi}\sum_{n=1}^{\infty}\frac{\cos(2n-1)(\frac{1}{2}\pi a|s-t|/b) - \cos(2n-1)(\frac{1}{2}\pi a|s+t|/b)}{(2n-1)}. \qquad \text{(B.5)}$$

We note (e.g. Gradshteyn and Ryzhik [18, §1.442(2), §1.518(3)]) that

$$\sum_{n=0}^{\infty}\frac{\cos(2n-1)X}{(2n-1)} \approx -\frac{1}{2}\log(\tan(|X|/2)) \approx -\frac{1}{2}\log(|X|/2) - \frac{X^2}{24} \qquad \text{(B.6)}$$

for small $|X|$ and it follows that

$$S_2^a(as,at) \approx -\frac{1}{\pi}\log(|s-t|/|s+t|) + \frac{\pi a^2 st}{12b^2} \qquad \text{(B.7)}$$

as $a \to 0$. Returning to S_1^a we write

$$S_1^a(as,at) = S_{11}^a(as,at) + S_{12}^a(as,at)$$

where

$$S^a_{11}(as,at) = 2\sum_{n=0}^{\infty}\left(\frac{\coth\gamma^a_n c}{\gamma^a_n b} - \frac{1}{\alpha^a_n b} - \frac{\frac{1}{2}(kb)^2}{(\alpha^a_n b)^3}\right)\sin(\alpha^a_n as)\sin(\alpha^a_n at) \quad \text{(B.8)}$$

and

$$S^a_{12}(as,at) = \frac{4(kb)^2}{\pi^3}[W(\tfrac{1}{2}\pi a(s-t)/b) - W(\tfrac{1}{2}\pi a(s+t)/b)] \quad \text{(B.9)}$$

in which

$$W(X) = \sum_{n=1}^{\infty}\frac{\cos(2n-1)X}{(2n-1)^3}.$$

Now we only need to determine the behaviour of $W(X)$ for small X and we note that integrating (B.6) twice respect to X gives

$$W(X) \approx \frac{7}{8}\zeta(3) + \frac{1}{4}X^2\ln(|X|/2) - \frac{3}{8}X^2.$$

Thus we have from (B.9)

$$\begin{aligned} S^a_{12}(as,at) \;\approx\; & \frac{3k^2a^2}{2\pi}st \\ & + \frac{k^2a^2}{4\pi}\left((s^2+t^2)\ln\left(\frac{|s-t|}{|s+t|}\right) - 2st\ln\left(\frac{\pi^2a^2|s^2-t^2|}{16b^2}\right)\right) \end{aligned} \quad \text{(B.10)}$$

as $a \to 0$.

Bringing all the results (B.4), (B.7), (B.10) above together with (B.8) which can be expanded to $O(a^2)$ we find that

$$L^a(as,at) \approx -\frac{2}{\pi}\ln(|s-t|/|s+t|) + a^2G(s,t) \quad \text{(B.11)}$$

where

$$G(s,t) = A^a st + \frac{k^2}{2\pi}\left((s^2+t^2)\ln\left(\frac{|s-t|}{|s+t|}\right) - 2st\ln|s^2-t^2|\right) \quad \text{(B.12)}$$

with

$$\begin{aligned} A^a \;=\; & \frac{3k^2}{\pi} - \frac{k^2}{\pi}\ln\left(\frac{\pi^2a^2}{4b}\right) + \frac{\pi}{12b^2} + \frac{\pi}{6} \\ & + \frac{2}{b^2}\sum_{n=0}^{\infty}\left(\frac{(\alpha^a_n b)^2\coth\gamma^a_n c}{\gamma^a_n b} - \alpha^a_n b - \frac{(kb)^2}{2\alpha^a_n b}\right). \end{aligned} \quad \text{(B.13)}$$

References

[1] J.W. Strutt (Lord Rayleigh), On the theory of resonance, Phil. Trans. R. Soc. Lond. 161 (1871) 77–118.

[2] L.E. Kinsler, A.R. Frey, A.B. Coppens, J.V. Sanders, Fundamentals of Acoustics, fourth ed. John Wiley and Sons, 2000.

[3] R.C. Chanuad, Effects of geometry on the resonance frequency of Helmholtz resonators, J. Sound Vib. 178(3) (1994) 337–348.

[4] K.T. Chen, Y.H. Chen, K.Y. Lin, C.C. Weng, The improvement on the transmission loss of a duct by adding Helmholtz resonators, Appl. Acoustics 54(1) (1998) 71–82.

[5] C.G. Montgomery, R.H. Dicke, E.H. Purcell (Eds), Principles of Microwave Circuits, Peter Peregrinus Ltd, London, 1987.

[6] Z. Shao, W. Porod, C.S. Lent, Transmission resonances and zeros in quantum waveguide systems with attached resonators, Phys. Rev. B. 49(11) (1994) 7453–7465.

[7] Y. Xu, Y. Li, R.K. Less, A. Yariv, Scattering-theory analysis of waveguide-resonator coupling Phys. Rev. B. 62(5) (2000) 7389–7404.

[8] R.W. Scharstein, Complex resonances of a hard rectangular cavity coupled to a half-space through a narrow aperture, IEEE. Trans. Antennas Propag. 57(12) (2009) 3835–3846.

[9] C.C. Mei, The Applied Dynamics of Ocean Surface Waves, World Scientific Publishing Co. Pte. Ltd, 1989.

[10] O. Richoux, V. Pagneaux, Acoustic characterization of the Hofstadter butterfly with resonant scatterers, Europhys. Lett., 59(1) (2002) 34–40.

[11] N. Fang, D. Xi, J. Xu, M. Ambati, W. Srituravanich, C. Sun, X. Zhang, Ultrasonic metamaterials with negative modulus, Nature materials 5 (2006) 452–456.

[12] Z.G. Wang, S.H. Lee, C.K. Kim, C.M. Park, K. Nahm, S.A. Nikitov, Acoustic wave propagation in one-dimensional phononic crystals containing Helmholtz resonators, J. Appl. Phys. 103 (2008) 064907.

[13] Y.M. Seo, J.J. Park, S.H. Lee, C.M. Park, C.K. Kim, S.H. Lee, Acoustic metamaterial exhibiting four different sign combinations of density and modulus, J. Appl. Phys. 111 (2012) 023504.

[14] C. Faure, O. Richoux, S. Félix, V. Pagneaux, Experiments on metasurface carpet cloaking for audible acoustics, Appl. Phys. Lett. **108** (2016) 064103.

[15] V. Romero-García, G. Theocharis, O. Richoux, A. Merkel, V. Tournat, V. Pagneux, Perfect and broadband acoustic absorption by critically coupled sub-wavelength resonators, Sci. Rep. 6:19518 (2016) doi: 10.1038/srep19519.

[16] N. Jiménez, V. Romero-García, V. Pagneux, J.-P. Groby, Quasi-perfect absorption by sub-wavelength acoustic panels in transmission using accumulation of resonances due to slow sound, (Under review) (2017).

[17] D.V. Evans, R. Porter, Total transmission of waves through narrow gaps in channels. Accepted for publication in Quart. J. Mech. Appl. Maths. (2017).

[18] I.S. Gradshteyn, I.M. Ryzhik, Table of Integrals, Series and Products, Academic Press, 1980.